Crystal structure and thermodynamic properties of the non-centrosymmetric $PrRu_4Sn_6$ caged compound

Michael O Ogunbunmi and André M Strydom

Highly Correlated Matter Research Group, Physics Department, University of Johannesburg, P. O. Box 524, Auckland Park 2006, South Africa.

E-mail: moogunbunmi@gmail.com, mogunbunmi@uj.ac.za

Abstract. $PrRu_4Sn_6$ is a tetragonal, non-centrosymmetric structure compound. It is isostructural to the extensively studied Kondo insulator $CeRu_4Sn_6$ which crystallizes in the YRu_4Sn_6-type structure with space group $I\bar{4}2m$. In this structure, the Pr atom fills the void formed by the octahedral Ru_4Sn_6 units which results in a tetragonal body-centred arrangement. Here we present reports on the physical and magnetic properties of $PrRu_4Sn_6$. The temperature dependences of specific heat, $C_p(T)$, electrical resistivity, $\rho(T)$, and magnetic susceptibility, $\chi(T)$, reveal the absence of a long-range magnetic ordering down to 2 K. $\chi(T)$ follows a Curie-Weiss behaviour above 100 K with an effective magnetic moment, $\mu_{\text{eff}} = 3.34\ \mu_B$/Pr and paramagnetic Weiss temperature, $\theta_p = -19.47$ K indicating a dominant antiferromagnetic interaction. The magnetization at 2 K is quasi-linear in nature and attains a value of 0.86 μ_B/Pr at 7 T which is well reduced compared to the calculated value of 3.32 μ_B/Pr expected for a free Pr^{3+} ion. This is attributed to possible magneto-crystalline anisotropy in the system. $C_p(T)$ indicates the presence of a optical-phonon mode which is supported by a glass-like thermal conductivity above $\sim$45 K. This observation is associated with caged structured compounds where the low-frequency optical-phonon mode of the guest atom interacts with the host lattice, resulting in the scattering of heat-carrying quasiparticles.

1. Introduction

The $R Ru_4Sn_6$ (R = Y, La-Nd, Sm, Gd-Ho) series are intermetallic compounds which crystallize in the tetragonal YRu_4Sn_6-type structure with a non-centrosymmetric space group $I\bar{4}2m$ (No. 121) [1]. The structure was first reported by Venturini *et al* [2]. The crystal structure is made up of an octahedral Ru_4Sn_6 unit enclosing the guest R atom. Crystal structures of this nature have generated much interest lately especially in the search for new superconductors [3, 4]. Also, the non-centrosymmetric nature of the space group is characteristic of certain superconductors where the mixing of the spin-singlet and spin-triplet Cooper pairing channels have been found to give rise to a two-component order parameter [5–7]. $CeRu_4Sn_6$ is a Kondo insulator, and it is the most extensively studied member of the series [8–11]. Other studies by Koch and Strydom reveal a magnetic ordering for the isostructural compounds of $R Ru_4Sn_6$, with R = Sm, Gd and Dy compounds at low temperatures while those of Nd, Tb and Ho compounds are paramagnetic down to 2 K [12].

As part of our search for Pr-based systems exhibiting novel ground states, we have synthesized a polycrystalline sample of $PrRu_4Sn_6$ and investigated its physical and magnetic properties. It is noted that the existence of $PrRu_4Sn_6$ was first reported by Zumdick and Pöttgen [1] but no

physical or magnetic properties have been reported thereafter. The Pr atom in this structure has a tetragonal site symmetry of D_{2d} similar to those of the $Pr_3T_4X_{13}$ compounds, resulting in the crystal electric field splitting of the $J = 4$ multiplet into seven levels consisting of five singlets and two non-Kramers doublets.

2. Experimental methods

A polycrystalline sample of $PrRu_4Sn_6$ was prepared by arc melting stoichiometric amounts of high-purity elements (wt.% $\geq$ 99.9) on a water-cooled Cu plate under a purified static argon atmosphere in an Edmund Buehler arc furnace. The weight loss after melting was $\sim$ 0.05%. The arc-melted pellet was wrapped in Ta foil, placed in an evacuated quartz tube and annealed at 900°C for 21 days. A powder X-ray diffraction (XRD) pattern was recorded on a pulverized sample using a Rigaku diffractometer employing Cu-Kα radiation. The obtained powder XRD pattern was refined using the Rietveld method [13] employing the FullProf suite of programs [14]. We found that the compound was phase-pure within the limits of the resolution of the instrument. In Table 1, the atomic positions and lattice parameters obtained from the refinement are presented and are comparable with a previous report [1]. The refined XRD pattern and the crystal structure are shown in Fig. 1.

Magnetic properties were measured using the Magnetic Property Measurement System (Quantum Design Inc., San Diego) between 2 K and 300 K with an external magnetic field up to 7 T. The four-probe DC electrical resistivity, specific heat and thermal transport measurements between 2 K and 300 K were measured using the Physical Property Measurement System also from Quantum Design.

Table 1. The atomic positions and lattice parameters of $PrRu_4Sn_6$ obtained from a Rietveld refinement of the XRD pattern.

Site notation	Atom	Wyckoff site	Point symmetry	x	y	z
Sn(1)	Sn	8i	m	0.17635	0.17635	0.28771
Ru	Ru	8i	m	0.32788	0.32788	0.08126
Sn(2)	Sn	4c	222	0	1/2	0
Pr	Pr	2a	$-42m$	0	0	0
a (Å)	c (Å)	V (Å^3)	formula units (Z)	R_{wp} (%)	R_p (%)	χ^2
6.870(3)	9.761(2)	461.5(9)	2	8.588	7.295	5.210

3. Magnetic properties

The temperature dependence of magnetic susceptibility, $\chi(T)$, of $PrRu_4Sn_6$ in an external field of 0.1 T and in the temperature range of 2 K to 300 K is presented in Fig. 2. $\chi(T)$ shows a paramagnetic behaviour down to low temperatures with no indication of a long-range magnetic ordering observed. The white-solid line is a Curie-Weiss fit based on the expression: $\chi(T) = N_A\mu_{\rm eff}^2/(3k_B(T-\theta_p))$ for data above 100 K with values of effective magnetic moment, $\mu_{\rm eff}$ = 3.34 $\mu_{\rm B}$/Pr and Weiss temperature, $\theta_p = -19.47$ K. The observed $\mu_{\rm eff}$ is close to the calculated value of 3.58 $\mu_{\rm B}$/Pr expected for a free Pr^{3+} ion. At low temperatures, a Van-Vleck paramagnetic behaviour in $\chi(T)$ suggests a nonmagnetic ground state in $PrRu_4Sn_6$. The isothermal magnetization at 2 K is presented in the inset (b) of Fig. 2. The magnetization follows a quasi-linear behaviour up to 7 T and attains a value of 0.86 $\mu_{\rm B}$/Pr at 7 T which is well reduced compared to the saturation moment of 3.32 $\mu_{\rm B}$/Pr expected for a free Pr^{3+} ion implying a possible magneto-crystalline anisotropy in the compound.

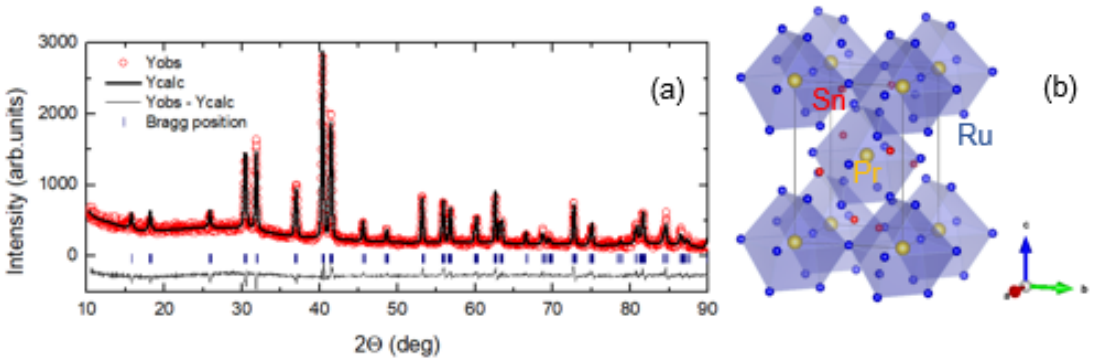

Figure 1. (a): Powder X-ray diffraction pattern of $PrRu_4Sn_6$ (red circles) with a Rietveld refinement (black line) based on the $I\bar{4}2m$ space group (No. 121). The vertical bars are the Bragg peak positions while the grey line represents the difference between the experimental and calculated intensities. (b): Crystal structure of $PrRu_4Sn_6$ showing Pr atom being enclosed by the Ru_4Sn_6 octahedral unit.

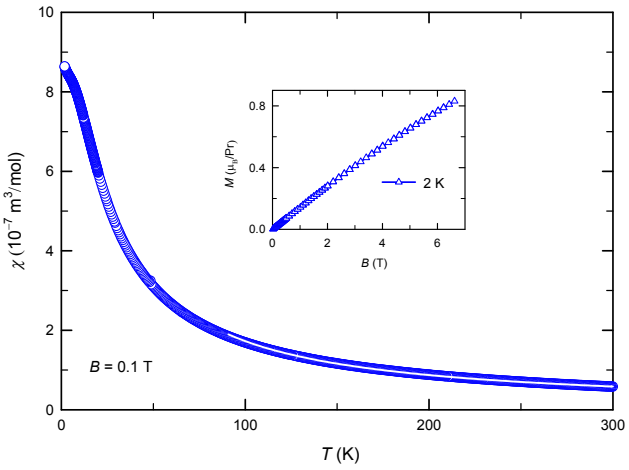

Figure 2. Temperature dependence of magnetic susceptibility, $\chi(T)$, of $PrRu_4Sn_6$ measured in a field of 0.1 T. The white-solid line is a Curie-Weiss fit described in the text. Inset (b): Isothermal magnetization of $PrRu_4Sn_6$ at 2 K.

4. Specific heat

The temperature dependence of specific heat, $C_p(T)$, of $PrRu_4Sn_6$ studied between 2 K and 300 K is presented in Fig. 3. Inset (a) of Fig. 3 shows a plot of C_p/T^3 against T. Such a plot is important in determining the possible presence of low-frequency Einstein modes in $C_p(T)$ through the occurrence of a local maximum in C_p/T^3. A local minimum is observed in the plot as indicated by the arrow at $T_{max} = 6$ K which confirms the presence of low-frequency Einstein modes in $PrRu_4Sn_6$. $T_{\max}$ is the temperature below which the Einstein modes are frozen out. By using a model incorporating both the Debye and Einstein terms, the experimental specific heat is fitted as shown by the red line in Fig. 3. The Debye-Einstein model is given by:

$$C_p(T) = mD\left(\frac{\theta_D}{T}\right) + nE\left(\frac{\theta_E}{T}\right), \tag{1}$$

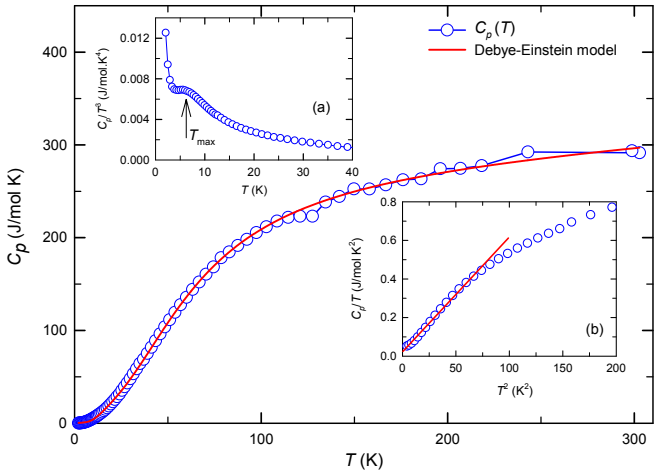

Figure 3. Temperature dependence of specific heat, $C_p(T)$, of $PrRu_4Sn_6$. Inset (a): Low-temperature plot of C_p/T^3 against T. Inset (b): Plot of C_p/T against T^2 along with a linear fit indicated by the red-solid line to extract the Sommerfeld coefficient.

$$D\left(\frac{\theta_D}{T}\right) = 9R\left(\frac{T}{\theta_D}\right)^3 \int_0^{\theta_D/T} \frac{x^4 \exp(x)}{(\exp(x)-1)^2} dx, \tag{2}$$

$$E\left(\frac{\theta_E}{T}\right) = 3R\left(\frac{\theta_E}{T}\right)^2 \cdot \frac{\exp\left(\theta_E/T\right)}{(\exp\left(\theta_E/T\right)-1)^2}, \tag{3}$$

where θ_D and θ_E are the Debye and Einstein temperatures with values of 241.73(9) K and 32.431(3) K, respectively. It is observed that $T_{max} \simeq 0.2\theta_E$ which is in agreement with the observation in $Ce_3Rh_4Sn_{13}$ [15]. In Inset (b), a plot of C_p/T against T^2 is shown together with a least-square fit (red line) based on the expression: $C_p/T = \gamma + \beta T^2$ and $\beta = 12\pi^4 nR/(5\theta_D^3)$, where n and R are the number of atoms per formula unit and universal gas constant, respectively, γ is the Sommerfeld coefficient and θ_D is the Debye temperature. Values obtained from the fit are: $\gamma = 38.60$ mJ/(K^2 mol) and $\theta_D = 154.50$ K. The γ observed for $PrRu_4Sn_6$ is about 10 times the values found in ordinary metals.

5. Transport properties

To further understand the physical properties of $PrRu_4Sn_6$, a thermal transport measurement was carried out between 2 K and 300 K. The temperature dependences of thermoelectric power, $S(T)$, and thermal conductivity, $\kappa(T)$, were measured simultaneously on a bar-shaped sample. As shown in Fig. 4 (a), $S(T)$ is positive throughout the temperature range investigated and attains a value of 18.81 μV/K at room temperature. The red and black-dashed lines suggest two areas of linear-in-T behaviour on either side of ~135 K. At 2 K, $S(T)$ has a value of ~1 μV/K indicating a significant drop in the carrier concentration between room temperature and 2 K. The change in slope of $S(T)$ at about 145 K is consistent with the anomaly observed in $C_p(T)$ around the same temperature. The origin of such an observation is not immediately clear and further measurements are needed to resolve the physics at play. A plot of $S(T)/T$ is shown in the inset of Fig. 4 (a). For $T \leq 100$ K the slope of $S(T)/T$ is ~ 0.7 μ V/K^2 which is slightly above those of ordinary metals. The general feature of $S(T)$ suggests a hole-type charge carriers near the Fermi level.

The total thermal conductivity, $\kappa_T(T)$, of $PrRu_4Sn_6$ is presented in Fig. 4 (b) on a log-log

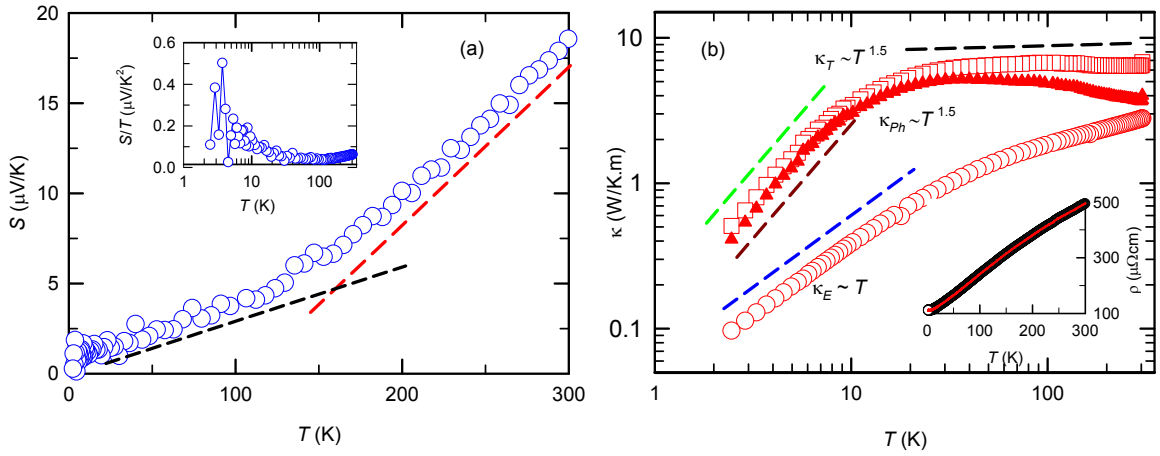

Figure 4. (a) Temperature dependence of thermoelectric power, $S(T)$, of $PrRu_4Sn_6$. The red and black-dashed lines are guides to the eye, indicating a change in slope of $S(T)$ at ∼145 K. Inset: Plot of S/T against T on a semi-log axis. (b) Temperature dependences of total thermal conductivity, $\kappa_T(T)$, phonon thermal conductivity, $\kappa_{Ph}(T)$ and electronic thermal conductivity, $\kappa_E(T)$. The green, brown and blue dashed-lines represent the power-law behaviours of $\kappa_T(T)$, $\kappa_{Ph}(T)$ and $\kappa_E(T)$, respectively while the black-dashed line is a guide to the eye described in the text. Inset: Temperature dependence of electrical resistivity with a BG fit (red line) described in the text.

axes. $\kappa_T(T)$ is nearly temperature independent from room temperature down to about 45 K (as shown by the black-dashed line) which is characteristic of a glassy behaviour in thermal conductivity. The observation of a glass-like thermal conductivity in a crystalline compound is often associated with caged systems. The low-frequency optical-phonon mode of the guest atom scatters heat-carrying quasiparticles thus leading to a reduction in lattice thermal conductivity. Using the Wiedemann-Franz relation [16] given as: $\kappa = L_0T/\rho(T)$, where L_0 is the Lorentz number given by: $L_0 = \pi^2k_B^2/3e^2 = 2.45 \times 10^{-8}$ WΩ/K^2, the electronic contribution to the thermal conductivity, $\kappa_E(T)$ is extracted and it is also presented in Fig. 4 (b). Also shown in the plot is $\kappa_{Ph}(T)$ obtained by subtracting $\kappa_E(T)$ from $\kappa_T(T)$. Below about 10 K, $\kappa_T(T)$ and $\kappa_{Ph}(T)$ show power-law behaviour of $T^{1.5}$ while $\kappa_E(T)$ is linear-in-T as indicated by the green, brown and blue-dashed lines. This indicates a good metallic behaviour. $\kappa_{Ph}(T) > \kappa_E(T)$ in the whole temperature range studied revealed that the heat transport is not charge-carrier dominated.

The temperature dependence of electrical resistivity, $\rho(T)$, of $PrRu_4Sn_6$ is presented in the inset of Fig. 4 (b) between 2 K and 300 K. $\rho(T)$ follows a typical metallic behaviour down to low temperature with residual resistivity ratio ≈ 5 which indicates a good crystalline quality. No signature of long-range magnetic or any type of ordering is observed in the temperature range studied in support of the observations in $\chi(T)$ and $C_p(T)$. To further understand the electrical transport properties of $PrRu_4Sn_6$, the Bloch-Grüneisen (BG) expression [17] was fitted to the data in the whole temperature range (shown as a red line). The BG expression is given as:

$$\rho(T) = \rho_0 + \frac{4K}{\Theta_R}\left(\frac{T}{\Theta_R}\right)^5 \int_0^{\Theta_R/T} \frac{x^5 dx}{(e^x - 1)(1 - e^{-x})}, \tag{4}$$

where ρ_0 is the residual resistivity due to defect scattering in the crystal lattice, K is the electron-phonon coupling constant and Θ_R is the resistivity Debye temperature. Values of $\rho_0 =$

102.8(2) $\mu\Omega$ cm, $K = 90.19(1)$ $\mu\Omega$ cm K, and $\Theta_R = 39.20(1)$ K are obtained from the least-square fit.This observation here further supports a metallic behaviour of $PrRu_4Sn_6$.

6. Conclusion

We have studied the physical and magnetic properties of the non-centrosymmetric $PrRu_4Sn_6$ compound. A paramagnetic ground state is inferred from the magnetic susceptibility results down to 2 K. The presence of low-frequency Einstein modes are observed in $C_p(T)$. This observation is further supported by the glass-like thermal conductivity for temperatures above 45 K. $S(T)$ undergoes a change in slope at $\sim$ 145 K, which is around the same temperature an anomaly in $C_p(T)$ is observed. Further measurements are expected to help clarify the origin of the observations in $C_p(T)$ and $S(T)$.

Acknowledgement

MOO acknowledges the UJ-URC bursary for doctoral studies in the Faculty of Science. AMS thanks the SA-NRF (93549) and UJ-URC for financial support.

References

[1] Zumdick M F and Pöttgen R 1999 *Z. Naturforsch. B* **54** 863

[2] Venturini G, El Idrissi B C, Maréché J F and Malaman B 1990 *Mater. Res. Bull.* **25** 1541

[3] Yamada A, Higashinaka R, Matsuda T D and Aoki Y 2018 *J. Phys. Soc. Jpn.* **87** 033707

[4] Winiarski M J, Wiendlocha B, Sternik M, Wiśniewski P, O'Brien J R, Kaczorowski D and Klimczuk T 2016 *Phys. Rev. B* **93** 134507

[5] Bauer E, Hilscher G, Michor H, Paul C, Scheidt E W, Gribanov A, Seropegin Y, Noël H, Sigrist M and Rogl P 2004 *Phys. Rev. Lett.* **92** 027003

[6] Bauer E, Khan R T, Michor H, Royanian E, Grytsiv A, Melnychenko-Koblyuk N, Rogl P, Reith D, Podloucky R, Scheidt E W, Wolf W and Marsman M 2009 *Phys. Rev. B* **80** 064504

[7] Okuda Y, Miyauchi Y, Ida Y, Takeda Y, Tonohiro C, Oduchi Y, Yamada T, Duc Dung N, D Matsuda T and Haga Y 2007 *J. Phys. Soc. Jpn.* **76** 044708

[8] Strydom A M, Guo Z, Paschen S, Viennois R and Steglich F 2005 *Physica B* **359-361** 293

[9] Brüning E M, Baenitz M, Gippius A A, Paschen S, Strydom A M and Steglich F 2006 *Physica B* **378-380** 839

[10] Brüning E M, Brando M, Baenitz M, Bentien A, Strydom A M, Walstedt R E and Steglich F 2010 *Phys. Rev. B* **82** 125115

[11] Sundermann M, Strigari F, Willers T, Winkler H, Prokofiev A, Ablett J M, Rueff J P, Schmitz D, Weschke E, Sala M M and Severing A 2015 *Sci. Rep.* **5** 17937

[12] Koch N E and Strydom A M 2008 *J. Magn. Magn. Mater.* **320** 128

[13] Thompson P, Cox D E and Hastings J B 1987 *J. Appl. Crystallogr.* **20** 79

[14] Rodriguez-Carvajal J 1993 *Physica B* **192** 55

[15] Köhler U, Pikul A P, Oeschler N, Westerkamp T, Strydom A M and Steglich F 2007 *J. Phys. Condens. Matter* **19** 386207

[16] Kittel C 2004 *Introduction to Solid State Physics* 8th ed (Wiley, New York)

[17] Mott N F and Jones H 1958 *The Theory of the Properties of Metals and Alloys* (Dover publications, Inc., Oxford, England)